Pertanika J. Sci. & Technol. 33 (5): 2237 - 2258 (2025)

PERTANIKA JOURNALS

SCIENCE & TECHNOLOGY

Journal homepage: http://www.pertanika.upm.edu.my/

# Extraction and Characterisation of Leaf Fibres from *Pandanus atrocarpus, Pandanus amaryllifolius,* and *Ananas comosus*

**Syahril Amin Hashim[1], Been Seok Yew[1,2]*, Fwen Hoon Wee[3], Ireana Yusra Abdul Fatah[1], Nur Haizal Mat Yaakob[1] and Muhamad Nur Fuadi Pargi[1]**

[1]*Faculty of Innovative Design and Technology, Universiti Sultan Zainal Abidin, Gong Badak, 23100 Kuala Nerus, Terengganu, Malaysia*

[2]*Microfabrication, Sensor, Electronic and Computer System RG, Universiti Sultan Zainal Abidin, Gong Badak, 23100 Kuala Nerus, Terengganu, Malaysia*

[3]*Faculty of Electronic Engineering Technology, Universiti Malaysia Perlis, 02600 Arau, Perlis, Malaysia*

## ABSTRACT

*Pandanus atrocarpus*, *Pandanus amaryllifolius*, and *Ananas comosus* plants are abundantly found in Malaysia. This study reports on the water retting extracting leaf fibres method, the morphology, chemical structure (functional groups), thermal stability, and dielectric properties of the *P. atrocarpus*, *P. amaryllifolius*, and *A. comosus* leaf fibres. Morphological analysis showed that the average diameter of leaf fibres is 445.5 µm for *P. atrocarpus*, 226.3 µm for *P. amaryllifolius*, and 311.2 µm for *A. comosus*. The presence of hemicellulose, cellulose, and lignin in the leaf fibres was detected in Fourier transform infrared (FTIR) spectra. Thermogravimetric analysis (TG) indicates that the leaf fibres are thermally stable up to a temperature of 220°C. Differential thermogravimetric (DTG) and differential scanning calorimetry (DSC) curves revealed a consistent thermal behaviour of the leaf fibres, where hemicellulose and cellulose decomposed at 275.0 and 355.3°C, respectively. Incorporation of the leaf fibres from *P. atrocarpus*, *P. amaryllifolius*, and *A. comosus* into epoxy composites enhanced the dielectric properties performance of epoxy. Overall, the findings from this study suggest that the leaf fibres from *P. atrocarpus*, *P. amaryllifolius*, and *A. comosus* are potentially useful for diversifying polymerisation for high-frequency applications.

ARTICLE INFO

*Article history:*
Received: 18 November 2024
Accepted: 29 April 2025
Published: 28 August 2025

DOI: https://doi.org/10.47836/pjst.33.5.09

*E-mail addresses*:
syahrilamin@unisza.edu.my (Syahril Amin Hashim)
bseokyew@unisza.edu.my (Been Seok Yew)
fhwee@unimap.edu.my (Fwen Hoon Wee)
ireanayusra@unisza.edu.my (Ireana Yusra Abdul Fatah)
haizal@unisza.edu.my (Nur Haizal Mat Yaakob)
mohamadnurfuadi@unisza.edu.my (Muhamad Nur Fuadi Pargi)
* Corresponding author

*Keywords*: *Ananas* comosus, leaf fibres, *Pandanus amaryllifolius*, *Pandanus atrocarpus*

## INTRODUCTION

The utilisation of lignocellulosic fibres from plants as alternatives to synthetic fibres has gained significant attention due to their sustainability and renewability (Samuel et al., 2022; Yadav & Singh, 2022). Lignocellulosic

fibres consist of cellulose and amorphous constituents such as hemicelluloses, lignin, and impurities on the surface of the fibre, like pectin, waxes, and greases (Rana et al., 2021; Rao et al., 2023; Weerappuliarachchi et al., 2020). Cellulose is composed of linear macromolecular glucose chains in the form of microfibrils arranged in the plant cell wall. Hemicellulose contains microfibrils, which strengthen the fibres' structure, whereas lignin provides rigidity and decay resistance (Banagar et al., 2024; Diyana et al., 2024; Feng et al., 2024). There are four classifications of lignocellulosic fibres, namely leaf fibre, bast fibre, seed fibre, and agricultural residues. Incorporating lignocellulosic fibres has improved the strength and durability of composite materials, adsorbent fibres, and textile fibres (Diah et al., 2024; Elfaleh et al., 2023; Habibi et al., 2020; Meng et al., 2019; Owonubi et al., 2021; Yadav & Singh, 2022).

Pandanaceae family includes about 600 species and grows throughout the tropics of Asia. *Pandanus atrocarpus* (known as screw pine) and *Pandanus amaryllifolius* (known as fragrant pandan) are easily found and grow abundantly in Malaysia. *Pandanus atrocarpus* naturally grows in swampy and riverbank habitats. It has long, narrow, and sheathing leaves with parallel veins structure and spiny edges. *Pandanus atrocarpus* leaves have been widely used as thatching roofs and producing handicrafts. *Pandanus amaryllifolius* is widely planted at home as its scented leaves are commonly used in food and beverage flavouring (Azahana, Wikneswari, Noraini, Nordahlia et al., 2015; Hamdan et al., 2018; Hashim et al., 2023; Mohamed et al., 2018b). It has a similar long, narrow and parallel vein structure of leaves. In contrast, *Ananas comosu*s (pineapple) is a fruit-bearing plant. Despite belonging to Bromeliaceae family, it shares similar leaf characteristics with both *P. atrocarpus* and *P. amaryllifolius*, but it has waxy leaf surface. Traditionally, fibres are extracted from pineapple leaves to produce rope and textiles (Sethupathi et al., 2024).

Natural fibres can be incorporated as reinforcement in polymer composites, enhancing their tensile strength and thermal stability. Recent research emphasises the significance of *P. amaryllifolius* and *A. comosu*s leaf fibres compared to *P. atrocarpus*. Diyana et al. (2021, 2024) reported that *P. amaryllifoliu*s fibres contain high cellulose content (48.79%). Its fibres have been incorporated into polymer composites and yield impressive tensile strength up to 45.61 MPa (Diyana et al., 2021, 2024; Sari et al., 2019). Similarly, *A. comosus* fibres exhibit excellent tensile strength (up to 1620 MPa) and thermal stability, which have been commercially used as reinforcement in composites and the textile industry (Gaba et al., 2021; Hamzah et al., 2021; Mohd Ali et al., 2020; Neves et al., 2023; Prado & Spinacé, 2019; Santos et al., 2021; Sethupathi et al., 2024; Todkar & Patil, 2019). In contrast, the current research of *P. atrocarpus* leaf fibres primarily reports on their mechanical properties (Chin et al., 2018; Kuan et al., 2017; Mohamed et al., 2018a; Mohd Zain et al., 2024). It is essential to broaden the investigation on the characteristics of fibres extracted from *P. atrocarpus* leaf.

Natural fibres extracted from plants are potentially useful as conductive fillers for dielectric material. Dielectric material is used in high-frequency applications, commonly wireless and satellite communications, to suppress electromagnetic interference (EMI). Practically, metal is utilised to suppress EMI, but it is heavy, costly, and prone to corrosion, thus limiting its practical application. Consequently, polymeric-based dielectric material or conducting polymer is preferred as an alternative dielectric material to metal in EMI suppression. Polymeric-based dielectric material exhibits advantages such as being lightweight, highly flexible, and having excellent corrosion resistance (Wei et al., 2020; Yao et al., 2021; Zhang et al., 2018). However, it has low thermal conductivity, which causes poor heat dissipation efficiency (Chen et al., 2024). Polymer typically exhibits a single polarisation orientation within its molecules. To improve its thermal conductivity, conductive fillers such as metal, ceramic, and carbon are incorporated into polymer composites. The interaction of the conductive filler particles and polymer matrix facilitates polarisation behaviour, thus improving the overall dielectric properties and thermal conductivity (Gong et al., 2019; Kwon et al., 2021; Vallés et al., 2019; Wang et al., 2021; Yao et al., 2021; Zheng et al., 2024).

Natural fibers like *P. atrocarpus*, *P. amaryllifolius*, and *A. comosus* could serve as alternative conductive fillers to enhance the flow of electrical charges in the polymer composites for high-frequency applications (Al-Oqla et al., 2015; Tang et al., 2024). It is worth highlighting that while natural fibres can modify the properties of the polymer composites, they cannot entirely substitute polymer as the matrix. Studies have reported that natural fibres can be used to partially substitute the polymer matrix to reduce cost and enhance the properties of polymer composites. Polymer matrix has excellent adhesiveness and is generally used as a binding agent in composites, while natural fibres are used as fillers (Alazzawi et al., 2024; Elfaleh et al., 2023; Hao et al., 2018; Khalid et al., 2021; Sahari et al., 2013).

Since the species and growing environment may contribute to a diverse range of properties in the natural fibres, characterisation is crucial to investigate the quality and performance of the fibres. In this study, characterisation of the extracted fibres from the mature leaves of *P. atrocarpus*, *P. amaryllifolius*, and *A. comosus* was performed. The water retting method was carried out to extract the leaf fibres from the plants. The morphological properties, functional structure, and thermal properties of the extracted leaf fibres were analysed using scanning electron microscopy (SEM), Fourier transform infrared spectroscopy (FTIR), simultaneous thermogravimetric analyser (STA), and differential scanning calorimetry (DSC). An open-ended coaxial line method was used to measure the dielectric properties of the epoxy composites incorporated with extracted leaf fibres. Notably, the micromechanical characterisation is excluded in this study as the emphasis was placed on dielectric properties, as these parameters are crucial for high-frequency dielectric applications (Reddy et al., 2022; Singh et al., 2024; Xiong et al., 2025).

## MATERIALS AND METHODS

### Collection of Fibres

The collection of *P. atrocarpus*, *P. amaryllifolius*, and *A. comosus* leaves was conducted based on the maturity, age, and size in Kuala Nerus (Terengganu, Malaysia), as shown in Figure 1. It can be observed that *P. atrocarpus* and *P. amaryllifolius* leaves have parallel veins, while *A. comosus* has waxy surface leaves. The leaves of these plants were harvested from mature plants aged around 1 to 2 years, measuring approximately 5 cm in width.

(a)

(b)

(c)

*Figure 1*. (a) *Pandanus atrocarpus* plant and its leaf (parallel veins); (b) *Pandanus amaryllifolius* plant and its leaf (parallel veins); and (c) *Ananas comosus* plant and its waxy surface leaf

### Extraction of Leaf Fibres Using Water Retting

The water retting method was performed to extract the fibres from *P. atrocarpus*, *P. amaryllifolius*, and *A. comosus* leaves. The water retting method introduces moisture and natural enzymatic reaction that results from rotting bacteria and fungi for fibre extraction from the leaves. Water retting is a standard and preferred for its effectiveness in producing high-quality fibres (Diyana et al., 2021; Feleke et al., 2023; Plakantonaki et al., 2024). The stalks of *P. atrocarpus* and *P. amaryllifolius* leaves were separately soaked in stagnant water to undergo the water retting process at a room temperature of 20–25°C for 8 weeks (56 days), whereas the water retting process of *A. comosus* leaves was carried out for 4 weeks (28 days). The stagnant water emitted an unpleasant odour, and clean water needed to be replaced frequently (approximately every 2 to 3 days) during the water retting process. During the entire procedure, it became evident that the water retting process caused the soft tissue or gummy elements in the leaf stalk to dissolve and break down. The degumming of fibres from the retted leaf stalk is shown in Figure 2(a). This, in turn, facilitated the manual extraction of fibres by scraping and peeling them from the retted stalk of leaves, as shown in Figure 2(b). The extracted fibres were cleaned to

remove impurities and allowed to dry in a dehydrator at a temperature of 70°C for 12 hours. The extracted *P. atrocarpus*, *P. amaryllifolius*, and *A. comosus* leaf fibres are presented in Figures 2(c), 2(d), and 2(e), respectively.

In this study, water retting at standard room temperature (20–25°C) was found to be less efficient than at the optimal range of 30–32°C, slowing microbial activity and requiring longer stagnant time. However, extending the stagnant time can yield high-quality fibres. Conversely, water retting at 30–32°C produced fibres that were light, hard, and less durable (Aisyah et al., 2016; Różańska et al., 2023). *Pandanus atrocarpus* and *P. amaryllifolius* leaves require a longer stagnant time to dissolve the gummy elements of the leaves than *A. comosus* leaves. This is due to the structural differences in the leaves. The parallel vein structure of the *P. atrocarpus* and *P. amaryllifolius* leaves strengthens their durability. In contrast, *A. comosus* leaves have a less robust structure. Additionally, the sample collection involves mature and non-decorticated leaves, thus increasing the duration of stagnant water required to soften and dissolve the elements of the leaves during the water retting process.

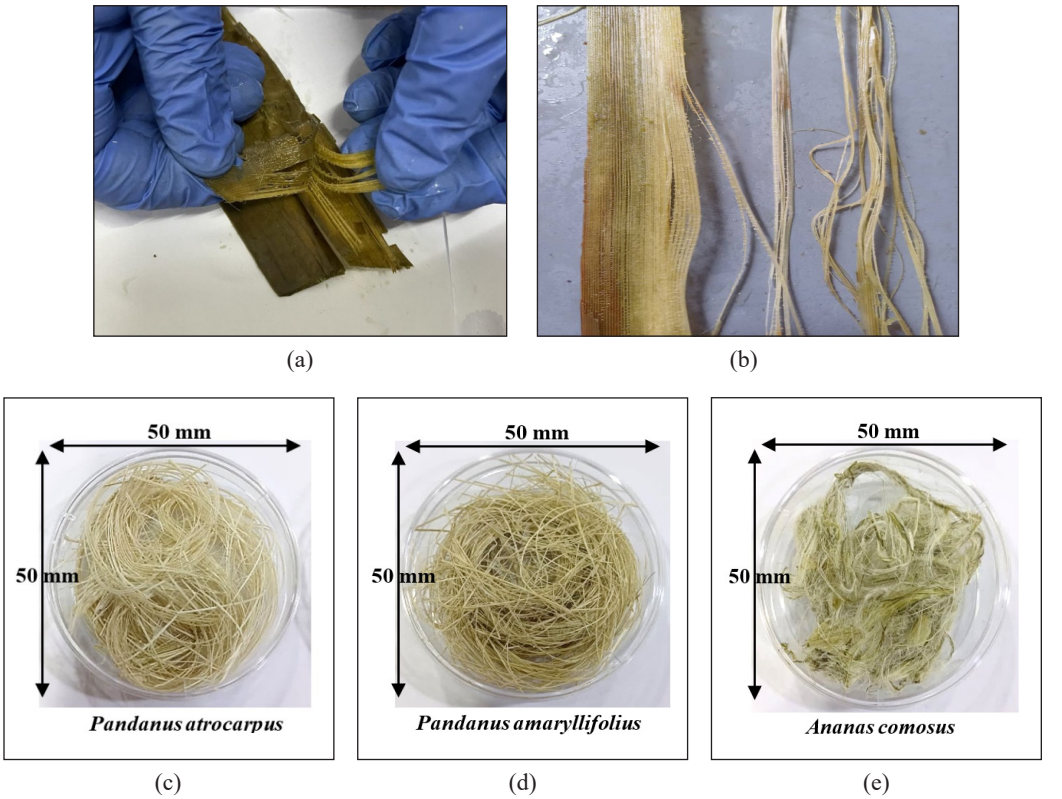


*Figure 2*. (a) Degumming the fibres from retted leaf stalk (*Pandanus atrocarpus*); (b) peeling of fibre; (c) extracted *P. atrocarpus* leaf fibres; (d) extracted *Pandanus amaryllifolius* leaf fibres; (e) extracted *Ananas comosus* leaf fibres

### Fibre Morphology and Diameter

The longitudinal fibre morphology and diameter of the leaf fibres were observed using Thermo Scientific Quattro Environmental Scanning Electron Microscope (ESEM, USA). The sample fibres were coated with a layer of 8 nm platinum using a G20 Ion Sputter Coater (GSEM Co., Ltd., South Korea) prior to characterisation to avoid electrostatic charges. The samples' fibres were observed at a magnification of 100×. The average diameter was randomly measured at different positions of each image, and the average value was determined.

### FTIR Spectroscopy Analysis

The infrared spectrum with percentage transmittance (%T) versus wavelength ($cm^{-1}$) was obtained by using a PerkinElmer Spectrum Two™ FTIR Spectrometer (USA) in attenuated total reflectance (ATR) mode within the range of 4000–450 $cm^{-1}$.

### Thermogravimetric Analysis (TGA) and Derivative Thermogravimetry (DTG)

The thermal stability of the leaf fibres was analysed through TGA and DTG using NETZSCH STA 2500 Regulus Simultaneous Thermal Analyser (Germany). Samples of 10 mg were scanned from 30 to 600°C. The heating rate temperature was 10°C/min with a constant nitrogen flow of 50 ml/min to avoid thermal oxidation**.**

### DSC

NETZSCH DSC 3500 Sirius DSC (Germany) was used to scrutinise the thermal transitions of the samples. Samples with a weight of 5–10 mg were heat scanned at a temperature range of 30–600°C under 40 ml/min nitrogen airflow and 10°C/min heating rate.

### Open-Ended Coaxial Line Method

An open-ended coaxial line method was used to measure the dielectric constant, dielectric loss factor and electrical conductivity over a wide microwave frequency range of 300 MHz-20 GHz at room temperature. For the open-ended coaxial line method, the dimension of the materials under test (MUT) must be > 20 mm and infinite thickness ≤ 5 mm to meet the requirement of open-ended coaxial probe dielectric properties measurement, to minimise the fringing field effect. The measurement apparatus includes an open-ended coaxial probe, an Agilent 85070E Dielectric Probe Kit (USA) and an Agilent E8362B PNA Series Network Analyser (USA). The MUTs were prepared by mixing the sample fibres with D.E.R.™ 331 epoxy resin and hardener (Euro Chemo-Pharma Sdn. Bhd., Malaysia). The extracted fibres were ground into short fibres using an IKA A10 Analytical Mill (Germany). It is recommended to ensure the fibre size is below 500 μm to minimise the risk of agglomeration and ensure better dispersion within the resin matrix (Callister

& Rethwisch, 2011). The composition of the MUT is 10% fibre to 90% matrix to avoid agglomeration, and is fabricated in a 50 mm diameter disposable petri dish with a thickness of 5 mm. Figure 3(a) presents the *P. atrocarpus* composite, Figure 3(b) shows the *P. amaryllifolius* composite, and Figure 3(c) displays the *A. comosus* composite, respectively.

The dielectric properties are presented in the form of complex permittivity ($\varepsilon$), dielectric constant ($\varepsilon'$), and dielectric loss factor ($\varepsilon''$), where $\varepsilon = \varepsilon' + \varepsilon''$. $\varepsilon'$ refers to the material's capacity to store electromagnetic (EM) energy, whereas $\varepsilon''$ indicates the ability to convert the stored EM energy into heat dissipation (heat loss). $\varepsilon''$ is always greater than zero and is much smaller than $\varepsilon'$. The ratio of heat dissipation to stored EM energy in a lossy material is known as the dissipation factor or tangent delta (tan $\delta$), where tan $\delta = \varepsilon''/\varepsilon'$ (Keysight Technologies, 2016).

Dielectric loss in materials measures energy dissipation as heat when an alternating electric field is applied. This loss is influenced by the material's dielectric properties and its conductivity. The relationship between dielectric loss and conductivity is $\sigma = 2\pi f \varepsilon_o \varepsilon''$, where $\sigma$ is the conductivity (S/m), $\varepsilon_o$ is the free space permittivity ($8.854 \times 10^{-12}$ F/m), $f$ is the frequency (Hz), ε" is the dielectric loss factor (Bouaamlat et al., 2020; Mittal et al., 2016). Materials with high conductivity will have higher dielectric losses, leading to more heat dissipation. This is crucial in applications like EMI shielding, where both the dielectric properties and conductivity of the material determine its effectiveness in absorbing and dissipating EM energy.

(a)

(b)

(c)

*Figure 3*. (a) *Pandanus atrocarpus* composite, (b) *Pandanus amaryllifolius* composite, and (c) *Ananas comosus* composite

## RESULTS AND DISCUSSION

### Fibre Morphology and Diameter

Samples of *P. atrocarpus*, *P. amaryllifolius*, and *A. comosus* leaf fibres were picked randomly to observe the longitudinal fibre morphology and to determine the average fibre diameter. It was observed that there is a presence of longitudinal streaks in the *P. atrocarpus*, *P. amaryllifolius*, and *A. comosus* leaf fibres' structure. The longitudinal fibre morphology showed that these fibres exhibit an arrangement of vertical alignments that follow the direction of the fibre axis, attributed to the compactly aligned microfibrils bonded together by lignin, pectin, and other non-cellulosic materials (Azahana, Wickneswari, Noraini, Nurnida et al., 2020; Donaldson et al., 2016; Hashim et al., 2023). The vascular bundle structure in

*P. atrocarpus* and *P. amaryllifolius* fibres can be easily detected and observed at 100× and 300× magnification, appearing as rectangular arrangements in the leaf fibres, contributing to the hydrophilic behaviour in the cellulosic fibres. It was observed that *P. atrocarpus* leaf fibres have a rougher surface texture than *P. amaryllifolius* and *Ananas comosus* leaf fibres. The fibre diameter of *P. atrocarpus* ranges from 421.0 to 458.7 µm, with average fibre diameter of 445.5 µm; whereas for *P. amaryllifolius*, the diameter ranges from 194.3 to 291.6 µm, with average fibre diameter of 226.3 µm; and for *A. comosus*, the diameter ranges from 258.5 to 393.9 µm, with average fibre diameter of 311.2 µm. The fibre diameters were measured randomly to account for the natural variability and irregularities in the fibres. The measured diameter of the natural fibres sample in this study aligns with findings from other research, supporting the consistency of these findings (Diyana et al., 2024; Gnanasekaran et al., 2022; Mohamed et al., 2018a; Neves et al., 2023; Kuan & Lee, 2014). The fibres' morphology of *P. atrocarpus*, *P. amaryllifolius*, and *A. comosus* leaves are presented in Figure 4.

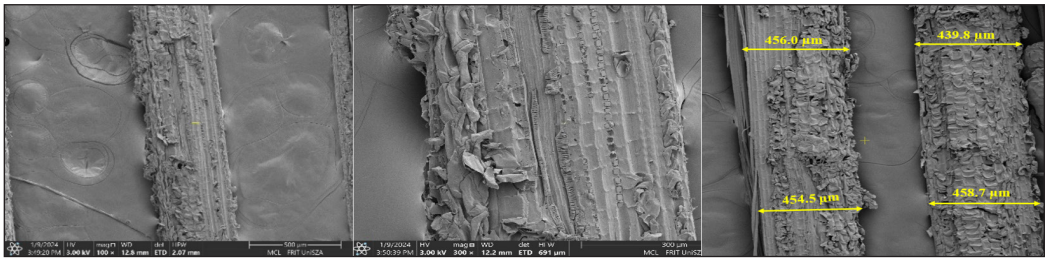


(a)

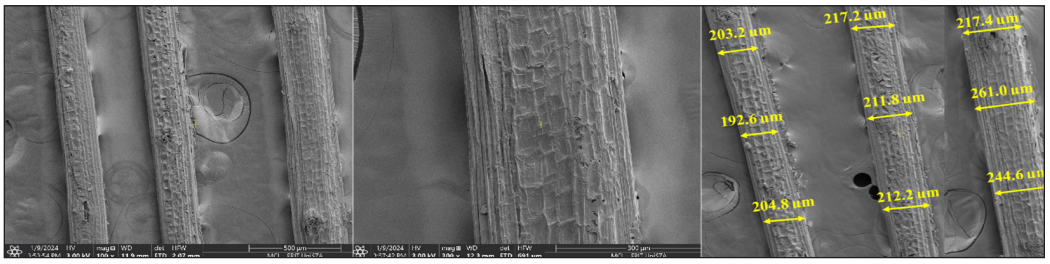


(b)

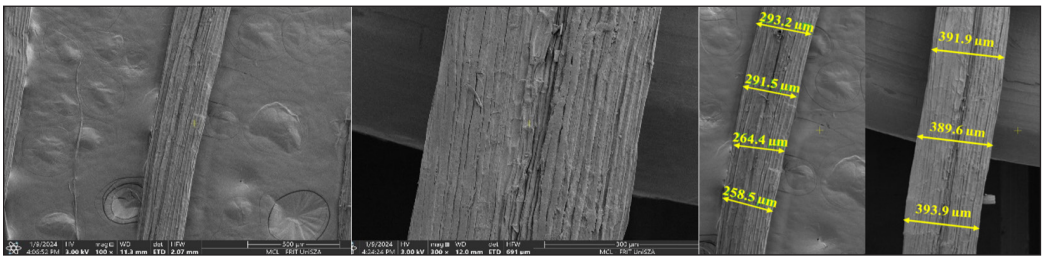


(c)

*Figure 4*. Scanning electron microscopy view of leaf fibres morphology (100× and 300× magnification) and diameter: (a) *Pandanus atrocarpus*, (b) *Pandanus amaryllifolius*, and (c) *Ananas comosus*

## FTIR Spectra Analysis

The FTIR spectra depicted in Figure 5 have been attributed to the lignocellulosic-based materials and verified the existence of cellulose, hemicellulose, and lignin in the *P. atrocarpus*, *P. amaryllifolius*, and *Ananas comosus* leaf fibres. The presence of the O-H stretching vibrations was observed at broad absorption peaks of 3330.88, 3340.21, and 3334.08 $cm^{-1}$, respectively, for *P. atrocarpus*, *P. amaryllifolius*, and *A. comosus* leaf fibres, which correlates to the hydrophilic hydroxyl group (OH) in cellulose, hemicellulose and lignin (Diyana et al., 2021; Shaker et al., 2020). The existence of cellulose and hemicellulose was confirmed by the absorption peaks observed at 2916.80, 2917.19, and 2916.53 $cm^{-1}$, corresponding to the alkanes C-H stretching (Ikhuoria et al., 2017; Ilyas et al., 2019; Yew et al., 2019). The sharp and intense C-H stretching peak observed in *P. atrocarpus* leaf fibre FTIR spectra implies that cellulose and hemicellulose are most dominant in *P. atrocarpus* leaf fibre compared to *P. amaryllifolius* and *A. comosus* leaf fibres (Md Salim et al., 2021).

The absorption peaks observed at 1731.20, 1729.51, and 1726.40 $cm^{-1}$ correspond to carbonyl C=O stretching vibrations of aliphatic carboxylic acids, acetyl and ketone groups in cellulose, hemicellulose and lignin (Alemdar & Sain, 2008; Diyana et al., 2021; Salem et al., 2021; Sheltami et al., 2012). The vibration of aromatic C=C further identifies

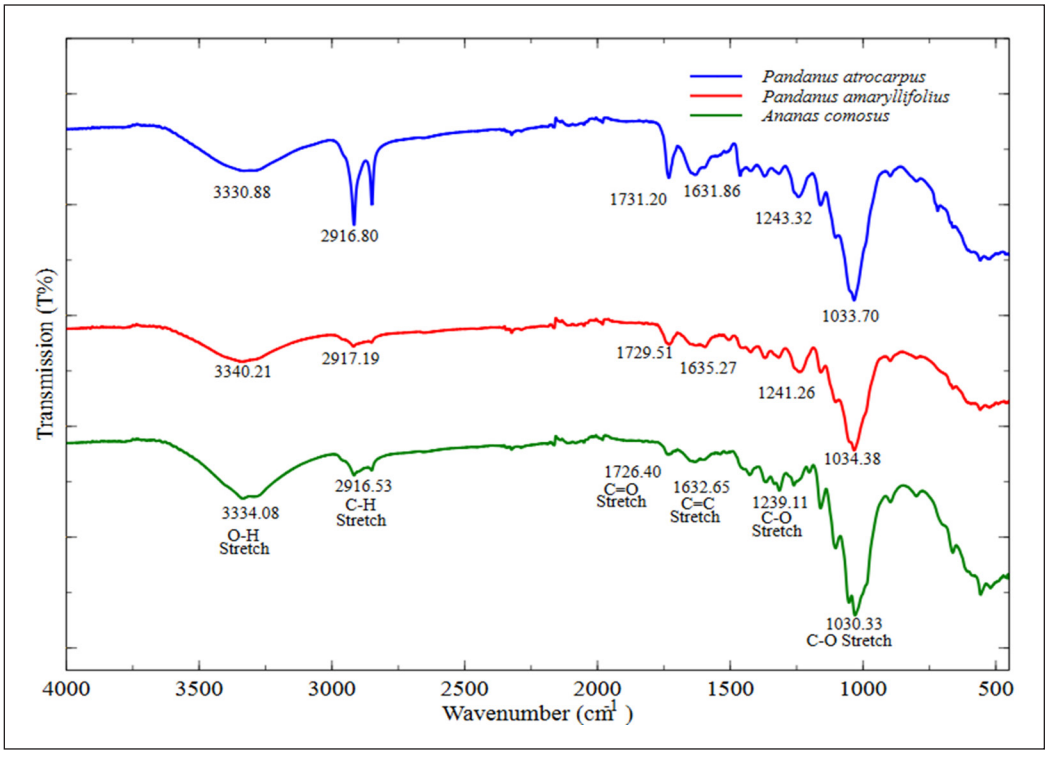


*Figure 5*. Fourier-transformed infrared spectra of the sample fibres

the presence of lignin rings functional groups detected at peaks 1631.86, 1635.27, and 1632.65cm$^{-1}$ (Shi et al., 2019). The aromatic ester linkage CO stretching vibration in ferulic carboxylic group, phenylpropanoids and p-coumaric acids in lignin and hemicellulose were observed at the absorption peaks of 1243.32, 1241.26, and 1239.65 cm$^{-1}$. The existence of C-O stretching corresponds to xylan-rich polysaccharide in cellulose and hemicellulose was further confirmed with the appearance of peaks at 1033.70, 1034.38, and 1030.33cm$^{-1}$ (Banagar et al., 2024; Diyana et al., 2021; Gaba et al., 2021).

## Thermal Analysis

### *TGA and DTG*

The thermal decomposition of natural fibre involves the dehydration, emission of volatile components, and weight loss due to lignocellulosic components degradation (Azwa et al., 2013; Yew et al., 2019). The degradation takes place in the following sequences: hemicellulose, cellulose, lignin, and the rest of the constituents (Tamanna et al., 2021). Figures 6(a) and 6(b) present the TG and DTG curves of the *P. atrocarpus*, *P. amaryllifolius*, and *A. comosus* leaf fibres. The curves showed that these samples' fibre degrade through four distinct stages in the following ranges: (I) from 30 to 120°C, (II) 120 to 220°C, (III) 220 to 390°C, and (IV) 390 to 600°C.

From Figures 6(a) and 6(b), the initial degradation occurs at range I, which marks the beginning of the weight loss in the sample fibres as the fibres were heated. The weight loss was attributed to the hydrophilic behaviour of the sample fibres, where evaporation of moisture and volatile contents occurred. The volatile contents tend to migrate to the fibre surface along with the movement of the water molecules from the internal parts to the outer surface of the fibre during the evaporation process. The moisture of the sample fibres was completely evaporated around 120°C with low mass loss of 7.27, 7.32, and 6.54%, respectively, for *P. atrocarpus*, *P. amaryllifolius*, and *A. comosus* leaf fibres.

The second stage of thermal degradation (Range II) started at temperatures above 120°C and was thermally stable until 220°C for all leaf fibres, where no significant peak of degradation is observed in both TG and DTG curves (Diyana et al., 2021; Ilyas et al., 2019; Ishak et al., 2012). At this stage, the average weight loss is about 0.6%, which is induced by the removal of impurities, waxes and inorganic components of volatile extractives from the fibres.

The third stage of thermal decomposition occurs at range III (200 to 390°C), corresponding to the degradation of hemicellulose and cellulose, resulting in significant mass loss up to 72%. As can be observed for *P. atrocarpus* and *P. amaryllifolius* fibres, two DTG peaks were observed on range III, which correspond to the degradation of hemicellulose that took place between 220 and 320°C. In contrast, the sharp DTG peaks can be observed at 320 to 390°C, corresponding to the degradation of cellulose. Hemicellulose structure is

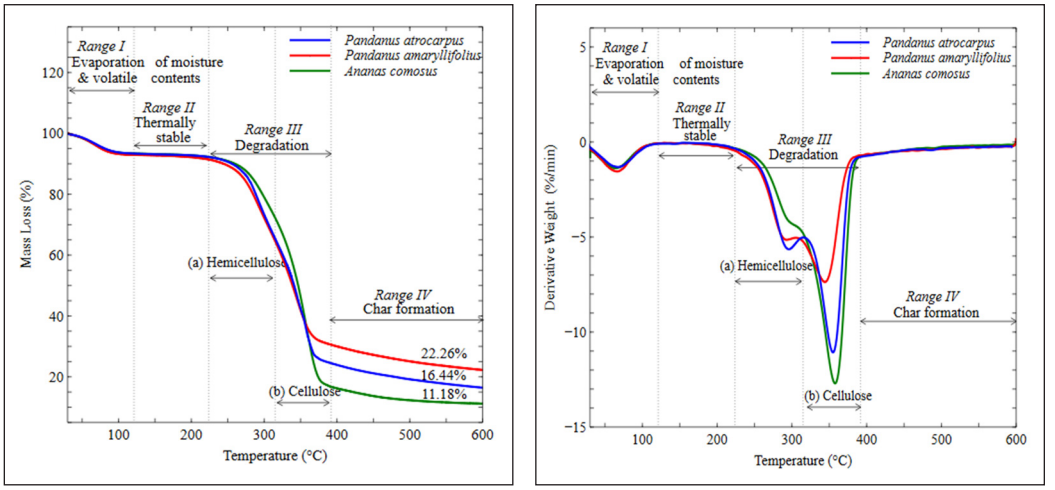


(a) (b)

*Figure 6*. (a) Thermogravimetry thermogram of weight loss as a function of temperature, and (b) derivative thermogravimetric curve of the rate of weight loss as a function of time

amorphous, which is less thermally stable and easily degrades to a volatile state at lower temperatures compared to cellulose. Cellulose structure is highly crystalline and thermally stable due to its microfibril chain cell wall. The highest peak of decomposition temperature in DTG occurred at 359.0, 355.9, and 344.2°C for *P. atrocarpus*, *P. amaryllifolius*, and *A. comosus* leaf fibre, respectively, attributed to the cellulose degradation.

The fourth stage decomposition that occurs up to 600°C at range IV corresponds to the degradation of lignin and the rest of the constituents in the sample fibres. The final residual is carbonaceous impurities, known as char. Char residue is 16.44, 22.26, and 14.04% respectively for *P. atrocarpus*, *P. amaryllifolius*, and *A. comosus* leaf fibres. The amount of residual weight obtained at the end of the combustion process in *P. amaryllifolius* was greater than that of *P. atrocarpus* and *A. comosus* leaf fibres. This indicates the highest thermal stability, attributed to a higher composition of char, suggesting improved fire resistance capability of the fibre, thus providing insulation against further thermal degradation. Furthermore, the char residue formation could be attributed to the presence of inorganic materials and silicon dioxide within the natural fibre. These components only degrade at extremely high temperatures exceeding 1,500°C (Diyana et al., 2024; Sahari et al., 2013).

## DSC Analysis

Natural fibre constituents (hemicellulose, cellulose, and lignin) are sensitive to temperature. When these fibre constituents are subjected to heat, separate peaks of decomposition can be detected. DSC is useful in assessing the thermal stability and composition of the natural fibres. DSC measures the temperature at which decomposition occurs. Higher

decomposition temperatures indicate better thermal stability and resistance to degradation, thus higher quality fibres (Acharya et al., 2024; PerkinElmer, 2011). Figure 7 shows the DSC curves of fibres from *P. atrocarpus*, *P. amaryllifolius*, and *A. comosus* leaves upon heating. The DSC curves clearly showed three distinct peaks. The presence of each peak represents the temperature at which the maximum rate of weight loss occurs, indicating the critical temperature at which the fibre composition decomposes.

The DSC curves showed a large and broad endothermic peak at the temperature range of 30–120°C (Range I), which indicates the removal of moisture by evaporation (volatilisation) in the intercellular region of the *P. atrocarpus*, *P. amaryllifolius*, and *A. comosus* leaf fibres. At the temperature range of 220–390°C (Range III), there were two peaks detected in the DSC curves. The exothermic peaks at a temperature range of 220–320°C represent the degradation of hemicellulose, where hemicellulose decomposed and produced char residue. Hemicellulose is an amorphous structure constituent that tends to absorb water as it consists of hydroxyl groups, which degrade earlier than cellulose and lignin. Cellulose is a crystalline structure constituent that possesses higher thermal stability than hemicellulose; thus, it exhibits higher degradation temperature. The endothermic peaks at a temperature range of 320–390°C represent the degradation of cellulose with the formation of volatiles. The extended temperature ranges from 390 to 600°C (Range IV) signifies the presence of lignin. The lignin curve showed a broad exothermic peak. Lignin possesses aromatic rings with many chemical branches. As a result, degradation

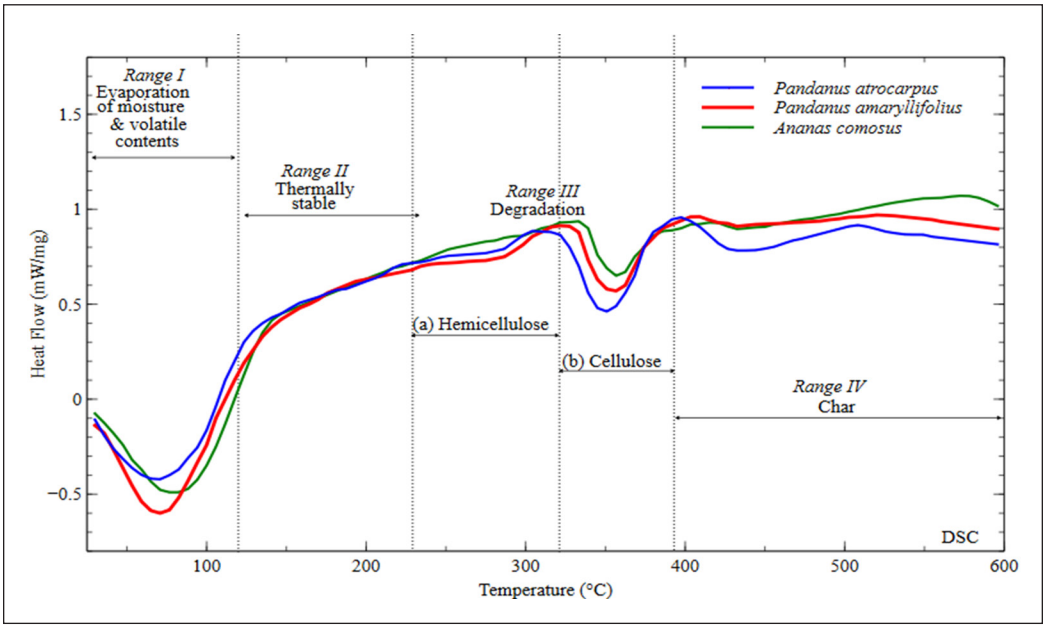


*Figure 7*. Differential scanning calorimetry curves of *Pandanus atrocarpus*, *Pandanus amaryllifolius*, and *Ananas comosus* leaf fibres

of lignin occurs over a broad temperature range. It might be attributed to the cracking of some functional groups in cellulose residue.

The DSC curves of the three leaf fibres corresponded well with their DTG curves. Hemicellulose and cellulose peaks in DSC curves appeared at around 275.0 and 355.3°C, respectively. The highest peak of decomposition temperature in DTG curves occurred at 359.0, 355.9, and 344.2°C for *P. atrocarpus*, *P. amaryllifolius*, and *A. comosus* leaf fibres, respectively, attributed to the cellulose degradation. These findings from the DSC curves in Figure 7 align with the DTG curves shown in Figure 6(b), where similar temperatures were observed for hemicellulose and cellulose.

**Dielectric Properties**

Figure 8(a) presents the dielectric constant, $\varepsilon'$, of the epoxy and composites filled with the sample fibres. It can be observed that over a wide range of frequencies up to 20 GHz, the $\varepsilon'$ of all composites is inversely proportional to the frequency at room temperature, with the $\varepsilon'$ trend decreasing as the frequency of the electromagnetic field increases. The $\varepsilon'$ is more significant at lower frequencies because the dipoles within the material have ample time to align with the alternating electric field, resulting in a higher dielectric constant. Conversely, at higher frequencies, the rapid oscillations of the electric field prevent the dipoles from fully orienting, thus leading to a decrease in the $\varepsilon'$ (Hassan & Ah-yasari, 2019). Figures 8(b)-(d), respectively, present the graphs of dielectric loss factor ($\varepsilon''$), dissipation factor (tan $\delta$), and conductivity ($\sigma$) versus frequency for all epoxy composites. Similar trends in the behaviour of $\varepsilon''$, tan $\delta$, and $\sigma$ were observed. At lower frequencies, the mechanism of energy dissipation in the epoxy composites increases with frequency as the polarization of the dipoles in the material is more effective in the electromagnetic field. This leads to higher energy dissipation as the dipoles continuously reorient themselves with the changing field, which increases the dielectric losses and conductivity, thus dissipating more heat. At higher frequencies (7.5 GHz onwards), the rapid oscillations of the electric field prevent the dipoles from fully aligning, leading to a decrease in these parameters. As a result, the ability of the dipoles to reorient decreases, leading to lower energy dissipation and a decrease in the $\varepsilon''$.

The comparative analysis using a two-sample t-test reveals statistically significant differences in the dielectric properties between the composites of *P. atrocarpus*, *P. amaryllifolius*, and *A. comosus* and epoxy. The p-values for all comparisons are less than the significance level of 0.05, and the t-scores are beyond the critical value of ±1.96, indicating that the results are statistically significant at the 95% confidence level. From the comparative analysis, epoxy without natural fibre filler shows slightly poorer dielectric properties compared to composites filled with *P. atrocarpus*, *P. amaryllifolius*, and *A. comosus* leaf fibres. While the relative differences indicate that epoxy has a higher dielectric constant in

each case (2.03% for *P. atrocarpus* composite, 1.92% for *P. amaryllifolius* composite, and 3.43% for *A. comosus* composite), these relative differences reflect that epoxy has better insulating properties, thus resulting in a higher dielectric constant in terms of heat storage. Consequently, its ability to dissipate heat is poorer, leading to a lower $\varepsilon''$, tan $\delta$, and $\sigma$.

When natural fibre fillers are added to epoxy, their chemical composition, which includes hemicellulose, cellulose, and lignin, captures and attracts charges due to interactions of polar molecules and displacement currents in the electromagnetic field. Hemicellulose contributes to flexibility and bonding within the epoxy composite, allowing the flow of

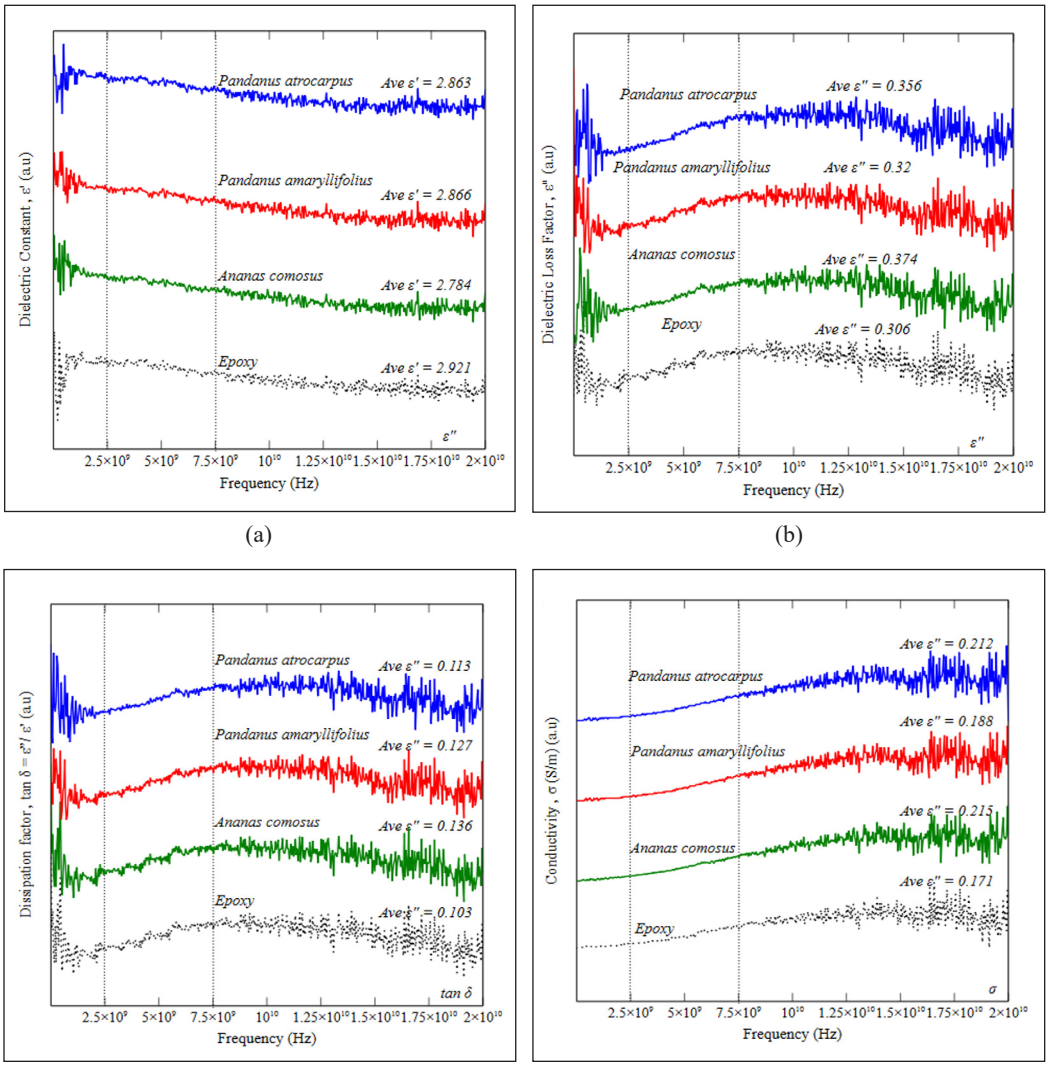


*Figure 8*. (a) The dielectric constant ($\varepsilon'$), (b) dielectric loss factor ($\varepsilon''$), (c) dissipation factor (tan $\delta$), and (d) conductivity ($\sigma$,) of the epoxy and composites filled with the sample fibres

displacement currents through the amorphous regions. The molecular structure of cellulose contributes to orientation polarization, thereby enhancing the material's ability to store and dissipate energy when subjected to an electromagnetic field. Lignin, with its complex aromatic structure, contributes to char formation and improves thermal stability, providing insulation against further thermal degradation (Rowlandson et al., 2020). Together, the fibres from *P. atrocarpus*, *P. amaryllifolius*, and *A. comosus* improve the overall dielectric behaviour of the epoxy composite by increasing orientation polarization, capturing charges, and promoting interaction with the electromagnetic field. It was observed that *A. comosus* composite exhibits higher relative differences in dielectric properties than *P. atrocarpus* and *P. amaryllifolius* composites. This can be attributed to the thermal stability of the *A. comosus* fibres that decompose more readily under thermal conditions, as confirmed by lowest mass residue and sharp peaks in TG and DSC curves, The differences in thermal stability between the natural fibres can influence the composite's overall dielectric response, as materials with different thermal stability can exhibits different polarization behaviours when subjected to an electromagnetic field (Airinei et al., 2021; Neto et al., 2021; Neves et al., 2023; Yusof et al., 2023).

## CONCLUSION

The leaf fibres extracted from *P. atrocarpus*, *P. amaryllifolius*, and *A. comosus* plants, exhibit potentially useful characteristics for a variety of high frequency applications as dielectric material for antennas, microwave circuits, and in electromagnetic interference (EMI) suppression to remove noise and improve signal quality. The fibres exhibit unique morphological features determined via SEM analysis. FTIR spectra reveal the existence of hemicellulose, cellulose and lignin constituents. Thermogravimetric analysis indicates that the fibres possess thermal stability up to 220°C. The consistent thermal behaviour was observed in both DTG and DSC curves, which further highlights the decomposition temperature peaks for hemicellulose and cellulose. The dielectric properties of the epoxy composites filled with natural fibres demonstrate better performance compared to epoxy. The addition of the *P. atrocarpus*, *P. amaryllifolius*, and *A. comosus* leaf fibres in the composites facilitates polarizations in the polymer composites. This approach aligns well with Sustainable Development Goals (SDGs) by encouraging innovation in sustainable materials by reducing the dependency on polymers (SDG 9), promoting greener and environmentally friendly materials (SDG 12), minimizing carbon footprint (SDG 13). To effectively use these natural fibres as fillers for polymer composites, it is crucial to address further their limitations on thermal stability, moisture resistance, and compatibility with the polymer matrix. This can be achieved through chemical treatments, surface modifications, or hybridization with compatibilizers to enhance the properties of natural fibres.

## ACKNOWLEDGEMENTS

The research conducted in this study was financially supported by Universiti Sultan Zainal Abidin, Malaysia, under the grant number UniSZA/2022/DPU2.0/25.

## REFERENCES

Acharya, P., Pai, D., Bhat, K. S., & Mahesha, G. T. (2024). Thermomechanical and morphological characteristics of cellulosic natural fibers and polymer based composites: A review. *Chemistry Africa*, *7*(10), 5149–5174. https://doi.org/10.1007/s42250-024-01157-0

Airinei, A., Asandulesa, M., Stelescu, M. D., Tudorachi, N., Fifere, N., Bele, A., & Musteata, V. (2021). Dielectric, thermal and water absorption properties of some EPDM/flax fiber composites. *Polymers, 13*(15), 2555. https://doi.org/10.3390/polym13152555

Al-Oqla, F. M., Sapuan, S. M., Anwer, T., Jawaid, M., & Hoque, M. E. (2015). Natural fiber reinforced conductive polymer composites as functional materials: A review. *Synthetic Metals*, *206*, 42–54. https://doi.org/10.1016/j.synthmet.2015.04.014

Alazzawi, S., Mahmood, W. A., & Shihab, S. K. (2024). Comparative study of natural fiber-reinforced composites for sustainable thermal insulation in construction. *International Journal of Thermofluids*, *24*, 100839. https://doi.org/10.1016/j.ijft.2024.100839

Alemdar, A., & Sain, M. (2008). Isolation and characterization of nanofibers from agricultural residues—Wheat straw and soy hulls. *Bioresource Technology*, *99*(6), 1664–1671. https://doi.org/10.1016/j.biortech.2007.04.029

Azahana, A., Wickneswari, R., Noraini, T., Nordahlia, A. S., Solihani, N. S., & Nurnida, M. K. (2015). Notes on *Pandanus atrocarpus* Griff and *P. tectorius* Parkinson in Peninsular Malaysia. In *AIP Conference Proceedings* (Vol. 1678, No. 1, p. 0200023). AIP Publishing. https://doi.org/10.1063/1.4931208

Azahana, A., Wickneswari, R., Noraini, T., Nurnida, K., Solehani, S., & Dahlia, A. S. (2020). Leaf anatomical and micromorphological adaptation of *Pandanus immersus* Ridley and *Pandanus tectorius* Parkinson. *Malayan Nature Journal*, *72*(3), 341–347.

Azwa, Z. N., Yousif, B. F., Manalo, A. C., & Karunasena, W. (2013). A review on the degradability of polymeric composites based on natural fibres. *Materials and Design*, *47*, 424–442. https://doi.org/10.1016/j.matdes.2012.11.025

Banagar, A. R., Patel, G. R. R., Srinivasa, C. V., Dhanalakshmi, S., Hemaraju, & Ramesh, B. T. (2024). Extraction and characterization of hemicellulose and lignin contents of areca fiber. *Journal of the Indian Academy of Wood Science*, *21*(1), 112–122. https://doi.org/10.1007/s13196-024-00330-9

Bouaamlat, H., Hadi, N., Belghiti, N., Sadki, H., Bennani M. N., Abdi, F., Lamcharfi, T., Bouachrine, M., & Abarkan, M. (2020). Dielectric properties, ac conductivity, and electric modulus analysis of bulk ethylcarbazole-terphenyl. *Advances in Materials Science and Engineering*, *2020*(1), 8689150. https://doi.org/10.1155/2020/8689150

Callister, W. D., & Rethwisch, D. (2011). *Materials science and engineering: An introduction*. John Wiley & Sons, Inc.

Chen, Q., Yang, K., Feng, Y., Liang, L., Chi, M., Zhang, Z., & Chen, X. (2024). Recent advances in thermal-conductive insulating polymer composites with various fillers. *Composites Part A: Applied Science and Manufacturing*, *178*, 107998. https://doi.org/10.1016/j.compositesa.2023.107998

Chin, S. C., Tong, F. S., Doh, S. I., Gimbun, J., Foo, Y. K., & Siregar, J. P. (2018). Potential external strengthening of reinforced concrete beam using natural fiber composite plate. *Applied Mechanics and Materials*, *878*, 41–48. https://doi.org/10.4028/www.scientific.net/AMM.878.41

Diah, S. B. M., Abdullah, S. H. Y. S., Seok, Y. B., Fatah, I. Y. A., Rahman, N. I. A., Hafizulhaq, F., & Alias, N. N. (2024). Towards sustainable food packaging: A review of thermoplastic starch (TPS) as a promising bioplastic material, its limitations, and improvement strategies with bio-fillers and essential oils. *Journal of Advanced Research in Fluid Mechanics and Thermal Sciences*, *119*(1), 80–104. https://doi.org/10.37934/arfmts.119.1.80104

Diyana, Z. N., Jumaidin, R., Selamat, M. Z., Alamjuri, R. H., & Yusof, F. A. M. (2021). Extraction and characterization of natural cellulosic fiber from *Pandanus amaryllifolius* leaves. *Polymers*, *13*(23), 4171. https://doi.org/10.3390/polym13234171

Diyana, Z. N., Jumaidin, R., Selamat, M. Z., Suan, M. S. M., Hazrati, K. Z., Yusof, F. A. M., Ilyas, R. A., & Eldin, S. M. (2024). Effect of *Pandanus amaryllifolius* fibre on physio-mechanical, thermal and biodegradability of thermoplastic cassava starch/beeswax composites. *Journal of Polymers and the Environment*, *32*(3), 1406–1422. https://doi.org/10.1007/s10924-023-03039-x

Donaldson, L., Nanayakkara, B., & Harrington, J. (2016). Wood growth and development. In B. Thomas, B. G. Murray & D. J. Murphy (Eds.), *Encyclopedia of applied plant sciences* (2nd ed., Vol. 1, pp. 203–210). Academic Press. https://doi.org/10.1016/B978-0-12-394807-6.00114-3

Elfaleh, I., Abbassi, F., Habibi, M., Ahmad, F., Guedri, M., Nasri, M., & Garnier, C. (2023). A comprehensive review of natural fibers and their composites: An eco-friendly alternative to conventional materials. *Results in Engineering*, *19*, 101271. https://doi.org/10.1016/j.rineng.2023.101271

Feleke, K., Thothadri, G., Tufa, H. B., Rajhi, A. A., & Ahmed, G. M. S. (2023). Extraction and characterization of fiber and cellulose from ethiopian linseed straw: Determination of retting period and optimization of multi-step alkaline peroxide process. *Polymers*, *15*(2), 469. https://doi.org/10.3390/polym15020469

Feng, Y., Hao, H., Lu, H., Chow, C. L., & Lau, D. (2024). Exploring the development and applications of sustainable natural fiber composites: A review from a nanoscale perspective. *Composites Part B: Engineering*, *276*, 111369. https://doi.org/10.1016/j.compositesb.2024.111369

Gaba, E. W., Asimeng, B. O., Kaufmann, E. E., Katu, S. K., Foster, E. J., & Tiburu, E. K. (2021). Mechanical and structural characterization of pineapple leaf fiber. *Fibers*, *9*(8), 51. https://doi.org/10.3390/fib9080051

Gnanasekaran, S., Ahamad Nordin, N. I. A., Jamari, S. S., & Shariffuddin, J. H. (2022). Isolation and characterisation of nanofibrillated cellulose from N36 *Ananas comosus* leaves via ball milling with green solvent. *Industrial Crops and Products*, *178*, 114660. https://doi.org/10.1016/j.indcrop.2022.114660

Gong, M., Sun, S.-G., Sun, L., Tian, A.-Q., & Li, Q. (2019). Simulation and experimentation of wide frequency electromagnetic shielding coating used for carbon fiber composite materials of track vehicles. *International Journal of Modern Physics B*, *33*(1–3), 1940020. https://doi.org/10.1142/S0217979219400204

Habibi, M., Selmi, S., Laperrière, L., Mahi, H., & Kelouwani, S. (2020). Post-impact compression behavior of natural flax fiber composites. *Journal of Natural Fibers*, *17*(11), 1683–1691. https://doi.org/10.1080/15440478.2019.1588829

Hamdan, M. H. M., Siregar, J. P., Bachtiar, D., Rejab, M. R. M., & Cionita, T. (2018). Mechanical properties of mengkuang leave fiber reinforced low density polyethylene composites. In S. M. Sapuan, H. Ismail & E. S. Zainudin (Eds.), *Natural fibre reinforced vinyl ester and vinyl polymer composites—Development, characterization and applications* (pp. 181–196). Woodhead Publishing. https://doi.org/10.1016/B978-0-08-102160-6.00009-3

Hamzah, A. F. A., Hamzah, M. H., Che Man, H., Jamali, N. S, Siajam, S. I., & Ismail, M. H. (2021). Recent updates on the conversion of pineapple waste (*Ananas comosus*) to value-added products, future perspectives and challenges. *Agronomy*, *11*(11), 1630. https://doi.org/10.3390/agronomy11112221

Hao, L. C., Sapuan, S. M., Hassan, M. R., & Sheltami, R. M. (2018). Natural fiber reinforced vinyl polymer composites. In S. M. Sapuan, H. Ismail & E. S. Zainudin (Eds.), *Natural fibre reinforced vinyl ester and vinyl polymer composites—Development, characterization and applications* (pp. 27–70). Woodhead Publishing. https://doi.org/10.1016/B978-0-08-102160-6.00002-0

Hashim, S. A., Yew, B. S., Fatah, I. Y. A., Wee, F. H., & Abdullah, N. A. (2023). Leaf anatomical characteristics of the *Pandanus immersus* Ridley virgin fibres using Field Emission Scanning Electron Microscope (FESEM). *Malayan Nature Journal*, *75*(2), 267–278.

Hassan, D., & Ah-yasari, A. H. (2019). Fabrication and studying the dielectric properties of (polystyrene-copper oxide) nanocomposites for piezoelectric application. *Bulletin of Electrical Engineering and Informatics*, *8*(1), 52–57. https://doi.org/10.11591/eei.v8i1.1019

Ikhuoria, E. U., Omorogbe, S. O., Agbonlahor, O. G., Iyare, N. O., Pillai, S., & Aigbodion, A. I. (2017). Spectral analysis of the chemical structure of carboxymethylated cellulose produced by green synthesis from coir fibre. *Ciencia e Tecnologia Dos Materiais*, *29*(2), 55–62. https://doi.org/10.1016/j.ctmat.2016.05.007

Ilyas, R. A., Sapuan, S. M., Ibrahim, R., Abral, H., Ishak, M. R., Zainudin, E. S., Asrofi, M., Atikah, M. S. N., Huzaifah, M. R. M., Radzi, A. M., Azammi, A. M. N., Shaharuzaman, M. A., Nurazzi, N. M., Syafri, E., Sari, N. H., Norrrahim, M. N. F., & Jumaidin, R. (2019). Sugar palm (*Arenga pinnata (Wurmb.) Merr)* cellulosic fibre hierarchy: A comprehensive approach from macro to nano scale. *Journal of Materials Research and Technology*, *8*(3), 2753–2766. https://doi.org/10.1016/j.jmrt.2019.04.011

Ishak, M. R., Sapuan, S. M., Leman, Z., Rahman, M. Z. A., & Anwar, U. M. K. (2012). Characterization of sugar palm (*Arenga pinnata*) fibres tensile and thermal properties. *Journal of Thermal Analysis and Calorimetry*, *109*, 981–989. https://doi.org/10.1007/s10973-011-1785-1

Keysight Technologies. (2016). *Measuring dielectric properties using Keysight's materials measurement solutions*. https://www.keysight.com/zz/en/assets/7018-03896/brochures/5991-2171.pdf

Khalid, M. Y., Al Rashid, A., Arif, Z. U., Ahmed, W., Arshad, H., & Zaidi, A. A. (2021). Natural fiber reinforced composites: Sustainable materials for emerging applications. *Results in Engineering*, *11*, 100263. https://doi.org/10.1016/j.rineng.2021.100263

Kuan, H. T. N., & Lee, M. C. (2014). Tensile properties of *Pandanus atrocarpus* based composites. *Journal of Applied Science and Process Engineering*, *1*(1), 39–44. https://doi.org/10.33736/jaspe.158.2014

Kuan, H. T. N., Lee, M. C., Khan, A. A., & Sawawi, M. (2017). The low velocity impact properties of pandanus fiber composites. *Materials Science Forum*, *895*, 56–60. https://doi.org/10.4028/www.scientific.net/MSF.895.56

Kwon, Y. J., Park, J. B., Jeon, Y. P., Hong, J. Y., Park, H. S., & Lee, J. U. (2021). A review of polymer composites based on carbon fillers for thermal management applications: Design, preparation, and properties. *Polymers*, *13*(8), 1–15. https://doi.org/10.3390/polym13081312

Md Salim, R., Asik, J., & Sarjadi, M. S. (2021). Chemical functional groups of extractives, cellulose and lignin extracted from native *Leucaena leucocephala* bark. *Wood Science and Technology*, *55*, 295–313. https://doi.org/10.1007/s00226-020-01258-2

Meng, F., Wang, G., Du, X., Wang, Z., Xu, S., & Zhang, Y. (2019). Extraction and characterization of cellulose nanofibers and nanocrystals from liquefied banana pseudo-stem residue. *Composites Part B: Engineering*, *160*, 341–347. https://doi.org/10.1016/j.compositesb.2018.08.048

Mittal, G., Rhee, Y. K., & Park, J. S. (2016). The effects of cryomilling CNTs on the thermal and electrical properties of CNT/PMMA composites. *Polymers*, *8*(5), 169. https://doi.org/10.3390/polym8050169

Mohamed, W. Z. W., Baharum, A., Ahmad, I., Abdullah, I., & Zakaria, N. E. (2018a). Effects of fiber size and fiber content on mechanical and physical properties of mengkuang reinforced thermoplastic natural rubber composites. *BioResources*, *13*(2), 2945–2959. https://doi.org/10.15376/biores.13.2.2945-2959

Mohamed, W. Z. W., Baharum, A., Ahmad, I., Abdullah, I., & Zakaria, N. E. (2018b). Mengkuang fiber reinforced thermoplastic natural rubber composites: Influence of rubber content on mechanical properties and morphology. *Malaysian Journal of Analytical Sciences*, *22*(5), 906–913. https://doi.org/10.17576/mjas-2018-2205-19

Mohd Ali, M., Hashim, N., Abd Aziz, S., & Lasekan, O. (2020). Pineapple (*Ananas comosus*): A comprehensive review of nutritional values, volatile compounds, health benefits, and potential food products. *Food Research International*, *137*, 109675. https://doi.org/10.1016/j.foodres.2020.109675

Mohd Zain, N., Aris, M. A., Ja'afar, H., & Awang, R. A. (2024). Characterization of electrical and mechanical properties of *Pandanus atrocarpus* flexible organic-based substrate for microwave communication in ISM applications. *Journal of Materials Science: Materials in Electronics*, *35*, 1694. https://doi.org/10.1007/s10854-024-13453-z

Nabilah Huda A. H., Ramlah, M. T., Aida Isma, M. I., Siti Aishah, G., Nor Munirah, A., & Che Man, H. (2016). Polysulfone membrane nutrients reclamation tests for nutrients reclamation of kenaf retted wastewater. *Jurnal Teknologi*, *78*(1–2), 59–63. https://doi.org/10.11113/jt.v78.7261

Neto, J. S. S., de Queiroz, H. F. M., Aguiar, R. A. A., & Banea, M. D. (2021). A review on the thermal characterisation of natural and hybrid fiber composites. *Polymers*, *13*(24), 4425. https://doi.org/10.3390/polym13244425

Neves, P., dos Santos, V., Tomazello-Filho, M., Cabral, M. R., & Junior, H. S. (2023). Leaf anatomy and fiber types of Curaua (*Ananas comosus* var. *erectifolius*). *Cellulose*, *30*, 3429–3439. https://doi.org/10.1007/s10570-023-05107-w

Owonubi, S. J., Agwuncha, S. C., Malima, N. M., Shombe, G. B., Makhatha, E. M., & Revaprasadu, N. (2021). Non-woody biomass as sources of nanocellulose particles: A review of extraction procedures. *Frontiers in Energy Research*, *9*, 608825. https://doi.org/10.3389/fenrg.2021.608825

PerkinElmer. (2011). *Characterization of single fibers for forensic applications using high speed DSC*. https://perkinelmer.cl/wp-content/uploads/2018/05/Characterization-of-Single-Fibers-for-Forensic-Applications-Using-High-Speed-DSC.pdf

Plakantonaki, S., Kiskira, K., Zacharopoulos, N., Belessi, V., Sfyroera, E., Priniotakis, G., & Athanasekou, C. (2024). Investigating the routes to produce cellulose fibers from agro-waste: An upcycling process. *ChemEngineering*, *8*, 112. https://doi.org/10.3390/chemengineering8060112

Prado, K. S., & Spinacé, M. A. S. (2019). Isolation and characterization of cellulose nanocrystals from pineapple crown waste and their potential uses. *International Journal of Biological Macromolecules*, *122*, 410–416. https://doi.org/10.1016/j.ijbiomac.2018.10.187

Rana, A. K., Frollini, E., & Thakur, V. K. (2021). Cellulose nanocrystals: Pretreatments, preparation strategies, and surface functionalization. *International Journal of Biological Macromolecules*, *182*, 1554–1581. https://doi.org/10.1016/j.ijbiomac.2021.05.119

Rao, J., Lv, Z., Chen, G., & Peng, F. (2023). Hemicellulose: Structure, chemical modification, and application. *Progress in Polymer Science*, *140*, 101675. https://doi.org/10.1016/j.progpolymsci.2023.101675

Reddy, P. L., Deshmukh, K., & Pasha, S. K. K. (2022). Dielectric properties of epoxy/natural fiber. In S. M. Rangappa, J. Parameswaranpillai, S. Siengchin, & S. Thomas (Eds.), *Handbook of epoxy/fiber composites* (pp. 575–609). Springer. https://doi.org/10.1007/978-981-19-3603-6_23

Rowlandson, J. L., Woodman, T. J., Tennison, S. R., Edler, K. J., & Ting, V. P. (2020). Influence of aromatic structure on the thermal behaviour of lignin. *Waste and Biomass Valorization*, *11*, 2863–2876. https://doi.org/10.1007/s12649-018-0537-x

Różańska, W., Romanowska, B., & Rojewski, S. (2023). The quantity and quality of flax and hemp fibers obtained using the osmotic, water-, and dew-retting processes. *Materials*, *16*(23), 7436. https://doi.org/10.3390/ma16237436

Sahari, J., Sapuan, S. M., Zainudin, E. S., & Maleque, M. A. (2013). Mechanical and thermal properties of environmentally friendly composites derived from sugar palm tree. *Materials and Design*, *49*, 285–289. https://doi.org/10.1016/j.matdes.2013.01.048

Salem, K. S., Naithani, V., Jameel, H., Lucia, L., & Pal, L. (2021). Lignocellulosic fibers from renewable resources using green chemistry for a circular economy. *Global Challenges*, *5*(2), 2000065. https://doi.org/10.1002/gch2.202000065

Samuel, B. O., Sumaila, M., & Dan-Asabe, B. (2022). Manufacturing of a natural fiber/glass fiber hybrid reinforced polymer composite ($P_xG_yE^z$) for high flexural strength: An optimization approach. *The International Journal of Advanced Manufacturing Technology*, *119,* 2077–2088. https://doi.org/10.1007/s00170-021-08377-5

Santos, D. I., Martins, C. F., Amaral, R. A., Brito, L., Saraiva, J. A., Vicente, A. A., & Moldão-Martins, M. (2021). Pineapple (*Ananas comosus* L.) by-products valorization: Novel bio ingredients for functional foods. *Molecules*, *26*(11), 3216. https://doi.org/10.3390/molecules26113216

Sari, N. H., Sanjay, M. R., Arpitha, G. R., Pruncu, C. I., & Siengchin, S. (2019). Synthesis and properties of pandanwangi fiber reinforced polyethylene composites: Evaluation of dicumyl peroxide (DCP) effect. *Composites Communications*, *15*, 53–57. https://doi.org/10.1016/j.coco.2019.06.007

Sethupathi, M., Khumalo, M. V, Skosana, S. J., & Muniyasamy, S. (2024). Recent developments of pineapple leaf fiber (PALF) utilization in the polymer composites—A review. *Separations*, 11(8), 245. https://doi.org/10.3390/separations11080245

Shaker, K., Waseem Ullah Khan, R. M., Jabbar, M., Umair, M., Tariq, A., Kashif, M., & Nawab, Y. (2020). Extraction and characterization of novel fibers from *Vernonia elaeagnifolia* as a potential textile fiber. *Industrial Crops and Products*, *152*, 112518. https://doi.org/10.1016/j.indcrop.2020.112518

Sheltami, R. M., Abdullah, I., Ahmad, I., Dufresne, A., & Kargarzadeh, H. (2012). Extraction of cellulose nanocrystals from mengkuang leaves (*Pandanus tectorius*). *Carbohydrate Polymers*, *88*(2), 772–779. https://doi.org/10.1016/j.carbpol.2012.01.062

Shi, Z., Xu, G., Deng, J., Dong, M., Murugadoss, V., Liu, C., Shao, Q., Wu, S., & Guo, Z. (2019). Structural characterization of lignin from *D. sinicus* by FTIR and NMR techniques. *Green Chemistry Letters and Reviews*, *12*(3), 235–243. https://doi.org/10.1080/17518253.2019.1627428

Singh, P. P., Dash, A. K., & Nath, G. (2024). Dielectric characterization analysis of natural fiber based hybrid composite for microwave absorption in X-band frequency. *Applied Physics A*, *130*, 171. https://doi.org/10.1007/s00339-024-07331-y

Tamanna, T. A., Belal, S. A., Shibly, M. A. H., & Khan, A. N. (2021). Characterization of a new natural fiber extracted from Corypha taliera fruit. *Scientific Reports*, *11*, 7622. https://doi.org/10.1038/s41598-021-87128-8

Tang, D., Qu, R., Xiang, H., He, E., Hu, H., Ma, Z., Liu, G., Wei, Y., & Ji, J. (2024). Highly stretchable composite conductive fibers (SCCFs) and their applications. *Polymers*, *16*(19), Article 2710. https://doi.org/10.3390/polym16192710

Todkar, S. S., & Patil, S. A. (2019). Review on mechanical properties evaluation of pineapple leaf fibre (PALF) reinforced polymer composites. *Composites Part B: Engineering*, *174*, 106927. https://doi.org/10.1016/j.compositesb.2019.106927

Vallés, C., Zhang, X., Cao, J., Lin, F., Young, R. J., Lombardo, A., Ferrari, A. C., Burk, L., Mülhaupt, R., & Kinloch, I. A. (2019). Graphene/polyelectrolyte layer-by-layer coatings for electromagnetic interference shielding. *ACS Applied Nano Materials*, *2*(8), 5272–5281. https://doi.org/10.1021/acsanm.9b01126

Wang, Z., Meng, G., Wang, L., Tian, L., Chen, S., Wu, G., Kong, B., & Cheng, Y. (2021). Simultaneously enhanced dielectric properties and through-plane thermal conductivity of epoxy composites with alumina and boron nitride nanosheets. *Scientific Reports*, *11*, 2495. https://doi.org/10.1038/s41598-021-81925-x

Weerappuliarachchi, J. W. M. E. S., Perera, I. C., Gunathilake, S. S., Thennakoon, S. K. S., & Dassanayake, B. S. (2020). Synthesis of cellulose microcrystals (CMC)/nylon 6,10 composite by incorporating CMC isolated from *Pandanus ceylanicus. Carbohydrate Polymers*, *241*, 116227. https://doi.org/10.1016/j.carbpol.2020.116227

Wei, H., Cheng, L., & Shchukin, D. (2020). Effect of porous structure on the microwave absorption capacity of soft magnetic connecting network Ni/$Al_2O_3$/Ni film. *Materials*, *13*(7), 1764. https://doi.org/10.3390/ma13071764

Xiong, R., Hu, Y., Xia, A., Huang, K., Yan, L., & Chen, Q. (2025). A high-temperature and wide-permittivity range measurement system based on ridge waveguide. *Sensors*, *25*(2), 541. https://doi.org/10.3390/s25020541

Yadav, V., & Singh, S. (2022). A comprehensive review of natural fiber composites: Applications, processing techniques and properties. *Materials Today: Proceedings*, *56*(5), 2537–2542. https://doi.org/10.1016/j.matpr.2021.09.009

Yao, Y., Jin, S., Zou, H., Li, L., Ma, X., Lv, G., Gao, F., Lv, X., & Shu, Q. (2021). Polymer-based lightweight materials for electromagnetic interference shielding: A review. *Journal of Materials Science*, *56*(11), 6549–6580. https://doi.org/10.1007/s10853-020-05635-x

Yew, B. S., Muhamad, M., Mohamed, S. B., & Wee, F. H. (2019). Effect of alkaline treatment on structural characterisation, thermal degradation and water absorption ability of coir fibre polymer composites. *Sains Malaysiana*, *48*(3), 653–659. https://doi.org/10.17576/jsm-2019-4803-19

Yusof, N. A. T., Zainol, N., Aziz, N. H., & Karim, M. S. A. (2023). Effect of fiber morphology and elemental composition of *Ananas comosus* leaf on cellulose content and permittivity. *Current Applied Science and Technology*, *23*(6), 1–12. https://doi.org/10.55003/cast.2023.06.23.002

Zhang, L., Bi, S., & Liu, M. (2018). Lightweight electromagnetic interference shielding materials and their mechanisms. In M.-G. Han (Ed.), *Electromagnetic materials and devices*. IntechOpen. https://doi.org/10.5772/intechopen.82270

Zheng, S., Wang, Y., Wang, X., & Lu, H. (2024). Research progress on high-performance electromagnetic interference shielding materials with well-organized multilayered structures. *Materials Today Physics*, *40*, 101330. https://doi.org/10.1016/j.mtphys.2024.101330